JÓZEF DUBIŃSKI*[#], KRYSTYNA STEC*, MIROSŁAWA BUKOWSKA*

GEOMECHANICAL AND TECTONOPHYSICAL CONDITIONS OF MINING-INDUCED SEISMICITY IN THE UPPER SILESIAN COAL BASIN IN POLAND: A CASE STUDY

GEOMECHANICZNE I TEKTONOFIZYCZNE UWARUNKOWANIA SEJSMICZNOŚCI INDUKOWANEJ W GÓRNOŚLĄSKIM ZAGŁĘBIU WĘGLOWYM W POLSCE – STUDIUM PRZYPADKU

In the Carboniferous rock mass of the Upper Silesian Coal Basin, large changes in the geomechanical conditions often occur over relatively short distances. These conditions relate to rock properties that are primarily responsible for the occurrence of geodynamic phenomena in the rock mass. The main factor influencing the manifestation of these phenomena is tectonic stress developed during Variscan and subsequent Alpine orogenesis. This stress contributed to creating tectonic structures in the Carboniferous formations and influenced the properties of the rocks themselves and the rock mass they form. As a result of the action of the stresses, compaction zones (main stresses were compressive) were formed, along with zones in which one of the main stresses was tensile. For the compaction zones in the Carboniferous rocks, the following geomechanical parameters have been calculated: uniaxial compressive strength, Young's modulus and post-critical modulus. The local stress field was determined according to the focal mechanism in selected areas (Main and Bytom troughs) to characterize changes in geomechanical properties of the rocks that are responsible for high-energy tremors ($E \geq 10^6$ J, $M_L \geq 2.2$).

Keywords: geomechanical properties, mining induced seismicity, focal mechanism, local stress field

W Górnośląskim Zagłębiu Węglowym w górotworze karbońskim występuje często duża zmienność warunków geomechanicznych na względnie niewielkich odległościach. Warunki te odniesione do właściwości skał są w pierwszej kolejności odpowiedzialne za występowanie zjawisk geodynamicznych w górotworze. Głównym czynnikiem wpływającym na te właściwości są naprężenia tektoniczne rozwinięte podczas orogenezy warescyjskiej i alpejskiej. Naprężenia te uczestniczyły w tworzeniu struktur tektonicznych w górotworze karbońskim i oddziaływały na właściwości skał i całego górotworu. W wyniku takiego działania powstały strefy kompacji (gdzie główne naprężenia były ściskające) oraz strefy, w których jedno z naprężeń głównych było rozciągającym. Dla stref kompacji zostały określone takie parametry geomechaniczne jak: wytrzymałość na jednoosiowe ściskanie, moduł Younga i moduł pokrytyczny. Lokalne pole naprężeń wyrażone kierunkami naprężeń głównych wyznaczano na podstawie parametrów mechanizmu ognisk wstrząsów w rejonie niecki głównej i niecki bytomskiej i porównano z wyznaczonymi parametrami geomechanicznymi skał. Przeprowadzone analizy pozwalają na wniosko-

* CENTRAL MINING INSTITUTE, PLAC GWARKÓW 1, 40-166, KATOWICE, POLAND

Corresponding author: jdubinski@gig.eu

wanie, że mechanizm ognisk wysokoenergetycznych wstrząsów ($E \geq 10^6$ J, $M_L \geq 2.2$) w przybliżeniu odzwierciedla występujący w górotworze układ naprężeń, który miał wpływ na zróżnicowanie wartości parametrów geomechanicznych skał.

Słowa kluczowe: parametry geomechaniczne, górnicza sejsmiczność indukowana, mechanizm ogniska, lokalne pole naprężeń

1. Introduction

The Carboniferous rock mass in the Upper Silesian Coal Basin (USCB) in Poland is characterized by variable geological structure in terms of both stratigraphy and tectonics. Fold tectonics, disjunctive (block) tectonics, and fault-and-block tectonics during Variscan orogenesis dominate this region, along with tectonic stresses developed during Alpine orogenesis. More locally, the state of stress in the rock mass of the area has been shaped by crustal tectonic processes together with primary stresses such as gravitational stress caused by overlying rocks, and stresses resulting from mining activity.

The state of stress in a rock mass is related to the manifestation of phenomena such as seismic tremors and rockbursts, and according to some researchers, influences the geomechanical properties of the rock mass. It has been shown that, in the USCB, tremors in the rock mass occur in zones of tectonic compaction which have greater strength and elasticity because of the increased density of the rock mass (Goszcz, 1985). However, only the uniaxial compressive strength (UCS) was analyzed, while currently it is possible to study the post-critical properties via stiffness testing and the analysis of post-critical parameters of the stress-strain curve, such as drop modulus. The post-critical properties are directly related to the way in which destruction of rocks occurs because destruction takes place in a post-critical phase once critical stress has been exceeded (Bukowska, 2012). As yet, the geomechanical properties of Carboniferous rocks in the post-critical phase of the USCB have not been fully investigated in relation to tectonophysical conditions.

To evaluate the influence of local rock mass tectonics on the process and sources of tremors, the focal mechanisms were examined using seismic moment tensor inversion. This method has been used for many years to determine stress distribution during earthquakes. The analyses show that a focal mechanism of high energy tremors roughly reflects the local stress state in the rock mass, and the local stress field is conditioned by changes in the values of geomechanical parameters.

2. Influence of tectonic stresses on structures of the Upper Silesian Coal Basin

The USCB formed from the Moravo-Silesian Basin and contains a tectonic unit of Brunovistulicum terrane which consists of the Upper Silesian Block and the Brno Block. The USCB is located in the Upper Silesian Block, which is why its borders do not match the borders of the Brunovistulicum terrane (Buła et al., 2008). In the Upper Silesian Block, coal-bearing formations were deposited between the Namurian and Westphal ages, and initially had a paralic character, and then developed a limnic character.

Geophysical images of the Upper Silesian Block show a few distinctive blocks within its structure (Kotas, 1982) . The blocks have a sub-longitudinal arrangement, and are separated from each other by second-order discontinuities. Within the Upper Silesian Block, the following struc-

tures can be distinguished: Upper Silesian Trough, Upper Silesian Fold Zone, Moravo-Silesian Fold-and-Thrust Belt, Bielsko-Biała Dome, Rzeszotary Horst and Liplas Graben.

The structure and tectonic history of the USCB is diverse and was shaped mainly during the Leonian phase of Variscan orogenesis. The characteristic elements of Variscan orogenesis are strike-slip movements along fault zones in the deep-seated basement, with westbound sinistral transpression of the bedrock under the Bohemian Massif, and compression from the west. The western part was folded and uplifted under the influence of overthrusting of the Moravo-Silesian branch of the Variscan Belt from the west, with dextral strike-slip movement in the north and northeast. This dextral strike-slip also occurred in the zone along the northern deep fault zone of the Cieszyn Block, resulting in lowering of the basin. During Alpine orogenesis, new tectonic structures (faults and foredeeps) were formed, or old structures were rejuvenated. However, the influence of Alpine tectonic movements on Variscan structures in the basin has not been determined. This is because of the limited extent, both horizontal and vertical, of Triassic and Jurassic formations. Thus, there is limited stratigraphic documentation of the age of the structures and faults, which may have been generated between the Westphal and Upper Miocene Epoch.

Many authors have assumed that the majority of tectonic structures in the USCB were created in the Variscan during compression, or by a predominantly horizontal component of stress. The result of the compression, acting from the west, was the emergence of overthrust fold structures. The compression was released in the main overthrusts of the fold zone, and waned in the Orłowski overthrust which forms the eastern border of the USCB. Similarly, it is assumed here that most of the asymmetric and arched half-grabens, which cut sub-longitudinally through the structure of the main trough, formed in the Variscan compression and low order zones of discontinuity in the USCB. A number of the grabens show evidence of tensional structures, which suggest sinistral transpression of the blocks in the bedrock.

Generally, strike-slip movements occur during horizontal compression, and such movements in the Upper Silesian Trough are associated with formation of longitudinal inversion structures. As the structures have a distinctive influence on fold structure characteristics in the western part of USCB (Moravo-Silesian block), it is likely that they formed simultaneously from the same tectonic process. Differences in the processes which led to their formation result only from the direction of compression, given that compression in the zone of fold tectonics (Moravo-Silesian thrust-and-fold belt) acted on sedimentary cover from the west, and was modified by movements of basement blocks. In the Upper Silesian Basin, the movements of basement blocks played a decisive role in formation of the Carboniferous structures. The movements occurred under compression, caused by stresses from the south and southeast.

Tectonic research conducted in mining excavations has also shown the occurrence of vertical movement in the form of subsidence and epeirogenic movements, which have influenced the formation of tectonic structures in the basin (Goszcz, 1980). Dependencies between tectonic structures and stresses have been considered and analyzed by, amongst others (Anderson, 1951; Sanford, 1959; Kisiel, 1973; Gzowskij, 1975). The aim of these works was to analyze and determine the distribution of fault-related stresses, and to calculate the distribution of primary stress trajectories in blocks subjected to horizontal stress and uplift.

Theoretical analysis, and confirmatory tests, has formed the basis of tectonophysical map preparation of certain areas of the Upper Silesian Trough. Based on these maps and analysis of the distribution of the three principal stresses, the stress fields were determined, and it is expected that changes in the uniaxial compressive strength are evident in the Carboniferous rocks. The relationship amongst the dynamic elasticity modulus, dynamic Poisson's ratio, and tectonic

stresses in the USCB, in reference to the occurrence of certain geodynamic phenomena in the rock mass in USCB has been determined (Goszcz & Dworak, 1982).

Research into stress restoration based on focal mechanism is also very important. Teper (1998) developed a seismogenic model of the northern part of the USCB and were able to show that the state of the rock stresses reproduced from the analysis of the focal mechanism of high-energy tremors and the rock deformation system formed during the most recent orogenesis characterized by mutual similarity. In this model, the maximum compressive stress (σ_1) was generally horizontal, and the tensile minimum stress (σ_3) was also horizontal. The intermediate stress (σ_2) was mostly vertical.

Tectonic stresses generated in the USCB based on the focal mechanisms of strong, induced mining events have been researched by Marcak and Mutke (2013). The results showed that tectonic stresses, particularly horizontal stress components, were essential in the distribution of seismic tremors caused by reverse faulting (Kozłowska et al., 2016) also showed that the full moment tensor solution revealed that the strong mining events occurred on an almost vertical plane, consistent with the approximate strike of local tectonic structures.

3. Overview of mining-induced seismicity in the USCB recorded by the Upper Silesian Regional Seismological Network

Poland's Central Mining Institute has been observing mining-induced seismicity in collieries in the USCB since the 1950s. The monitoring was initially based on only a few single seismic stations, but since 1974 has evolved into the Upper Silesian Regional Seismological Network. Detailed characterization of seismic activity recorded in the USCB (1977-2015) by this network, which has been operating continuously since 1977, was presented in the papers Stec (2007) and Lurka i Stec (2015).

This paper provides a brief overview for the period 1977-2016 to preserve data continuity. A total of 62646 strong tremors with seismic energy (E) values $\geq 10^5$ J (local magnitude $M_L \geq 1.7$) were recorded in the USCB during this time (Fig. 1). Local magnitude M_L was calculated from seismic energy from local mine network recordings using the formula: $\log E = 1.8 + 1.9 M_L$ (Dubiński & Wierzchowska, 1973), where E is the seismic energy in Joules. During the 1977-2016 period 53260 events with seismic energies of 10^5 J ($1.7 \leq M_L < 2.2$) were recorded, 8433 with energies of 10^6 J ($2.2 \leq M_L < 2.7$), 850 tremors with energies of 10^7 J ($2.7 \leq M_L < 3.3$), and 85 with energies of 10^8 J ($3.3 \leq M_L < 3.8$). Only 17 events were recorded with energies of 10^9 J ($3.8 \leq M_L < 4.1$).

In the 1970s and 1980s the level of seismic activity in USCB was high compared with events in the 1990s and 2000s, with 2000-4000 seismic events recorded per year. This was also related to the high average number of rockbursts (20) per year. In subsequent years the number of tremors dropped significantly, to an average of 1000-1400 per year. This was also related to a decrease in the number of rockbursts (2 to 5 per year). The decline in the number of mine tremors and rockbursts was caused by decreased coal production and increase in seismic hazard prevention methods.

The sources of tremors are not evenly distributed in the USCB. Their occurrence is associated with five main areas that correspond to different geological units, especially in areas where coal seams are deeply buried, and where rock layers are characterized by layered sandstone
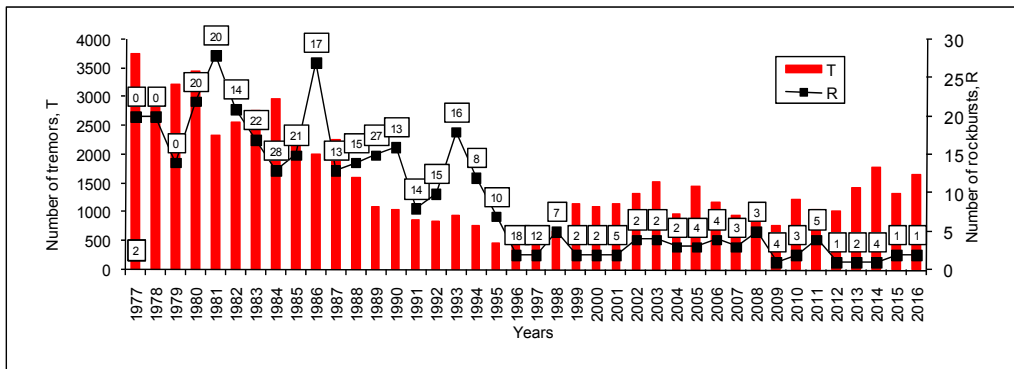
Fig. 1. Historical record of tremors with seismic energies $(E) \geq 10^5$ J $(M_L \geq 1.7)$ in the USCB

with well-developed tectonism. These five areas are referred to as: the Bytom trough, the main anticline, the main trough, the Kazimierz trough, the Jejkowice trough and the Jastrzębie folds. These areas have been subjected to significant seismic activity in the 1977-2016 period, as shown in Fig. 2 and Table 1.
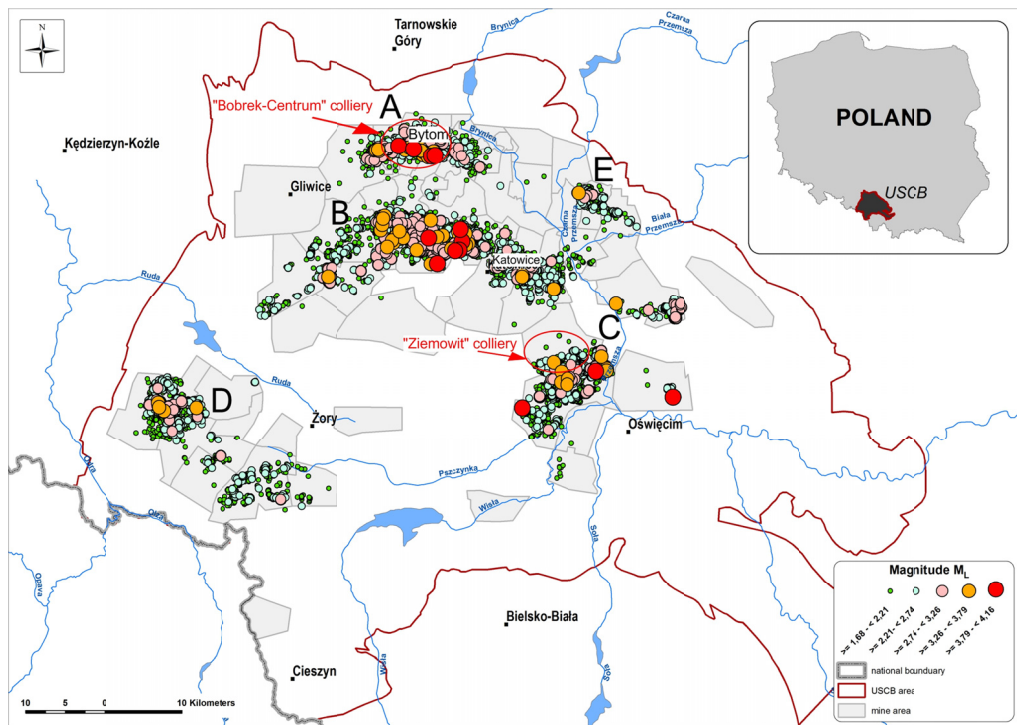

Fig. 2. Map of the USCB showing the epicenter locations of strong tremors $(M_L \geq 1.7)$ for the 1977-2016 period (A: Bytom trough, B: main anticline, C: main trough, D: Jejkowice trough and Jastrzębie folds, E: Kazimierz trough)

TABLE 1

Distribution of tremors in the five main geological units of the USBC during the period 1977-2016

Geological units	Number of tremors	Total energy (J)	Average energy (J)
Bytom trough	28532	6.22×10^{10}	2.32×10^6
Main anticline	16985	3.42×10^{10}	2.02×10^6
Main trough	7980	1.55×10^9	1.95×10^6
Jejkowice trough	6134	9.75×10^9	1.59×10^6
Kazimierz trough	3015	3.82×10^9	1.27×10^6

Table 1 and Fig. 3 show that the most seismically active area in the 1977-2016 period was Bytom trough, and the second-highest number of high-energy events was recorded in the main anticline. Seismic activity started in the main trough in the 1980s, with only a few tremors (13%) but with high average energy. The Jejkowice and Kazimierz troughs had the least number of tremors in the USCB: 10% and 5%, respectively.
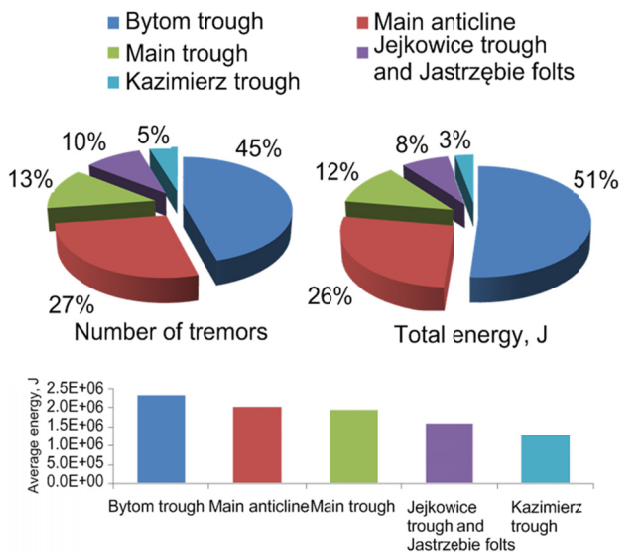

Fig. 3. Distribution of seismic tremors in the five main geological units in the USBC during the period 1977-2016

4. Case study areas

4.1. Calculation of the regional stress tensor

Changes in the properties of the Carboniferous rock mass, tectonic stress distribution and seismic tremors are important factors in the occurrence of multiple natural hazards. Such hazards include caving hazards, rockbursts (Bukowska, 2012), gas influx, water in rush (Bukowski & Augustyniak, 2013; Bukowski 2015) and seismic hazards (Kabiesz, 2016). The tectonic behavior

of the Upper Silesian Coal Basin is of great importance in the development of natural hazards, such as changes in the permeability of the rock mass and changes in coal quality and host rock behavior in fault zones in the USCB. Variable distribution of seismic activity throughout the USCB, as shown by many authors, is associated with variable distribution of geomechanical properties throughout the rocks, resulting in the influence of different stress fields during basin formation;). The seismic tremors occur in zones of tectonic compaction, and these zones have greater strength and elasticity because of increased rock density. These zones formed under the influence of adequate stress systems, with σ_1, σ_2 and σ_3 all being compressive, as determined from analysis of tectonic maps (Goszcz, 1985). In these zones, a higher level of seismic activity has been observed.

The stress field, which shaped fault tectonics in the main trough and Bytom trough, was modeled from parameters used to characterize fault azimuths from cleavage directions and the occurrence of complementary faults. After assuming a vertical direction for σ_1, and the direction of σ_2 parallel to the direction of the faults, it was possible to determine trajectories for σ_3. It was then possible to determine the zones in which all three principal stresses were compressive (compaction zones) and the state in which the minimum stress was tensile in four of the fault systems (Bukowska, 2009). These are referred to here as: System of meridional faults with N–S azimuth, System of faults II with SW–NE azimuth, System of longitudinal faults III with W–E azimuth and System of faults IV with NW–SE azimuth.

In this paper, the geomechanical properties of the Carboniferous rock mass are compared with the local stress field. The distribution of the mean stresses (azimuth and plunge) are calculated from the parameters of the focal mechanisms of high-energy tremors. Historically, the method for determining the stress tensor using earthquake focal mechanism data has been used to calculate the stress field in earthquake zones (McKenzie, 1969; Gephart & Forsyth, 1984; Michael, 1987; Angelier, 2002; Arnold & Townend, 2007; Fojtíková et al., 2010; Vavryčuk, 2014; Hofstetter et al, 2016). Given the similar origin of earthquakes, and mining-induced seismic tremors, this method was employed to analyze seismic activity in the USCB (Lurka & Stec, 2015; Stec, 2012; 2015). Based on the focal mechanism parameters, the locations of the destruction plane and the directions of displacement in the plane were determined for specific cases in which shear stress dominates the tremor sources. From these parameters it was then possible to determine the local stress field. The fundamental assumption of the method described by McKenzie (1969) is that the cracking process in the focus develops along a plane and the slip vector is parallel to shear stress in this plane. The calculation of such was made using MyFault software (Pangaea Scientific, Ontario Canada) based on the Minimized Principal Stress Variation method. This method was developed by Reches (1987) and assumes that the stress which causes fault slip obeys a Coulomb yield criterion ($\tau = C + \mu\sigma$) where τ is the shear stress that causes slip, C is the cohesive stress, μ is the friction coefficient and σ is the normal stress on the fault. From this relation, the principal stresses necessary for slip to occur can be determined. Assuming that all faults in the set were subject to the same regional stress state, the principal stresses should be the same for all faults. However, variations in material properties and other local effects will cause the actual stress state to vary between faults. To estimate the regional stress, it is assumed that the best value is found by minimizing the variation in the computed principal stresses within the fault set, using the same cohesion and friction coefficient for all faults. This assumption leads to an over-determined set of linear equations with values of C, μ and six principal stress components. The value of C is unknown and is assumed to be zero because the mean stress (hydrostatic or lithostatic stress), and hence the absolute normal stress, is unknown. All stresses are normalized

so that σ_1 is 1.0 and σ_3 is 0.0. Thus, the stress ratio (R) is equal to $(\sigma_2 - \sigma_3)/\sigma_1 - \sigma_3)$ and is equal to the value of σ_2. To find the value of the friction coefficient (μ), MyFault is used to solve the equations across a range of friction angles (0-45°), choosing the value that gives the minimum variation in principal stresses for all faults. Uncertainties in these quantities are estimated using the bootstrap resampling method (Michael, 1987; Reches, 1987).

The focal mechanism was calculated using the seismic moment tensor inversion method (SMT), in the time domain, from amplitudes and polarities of P-wave displacement onsets. Fundamentals of the SMT method have been described by Aki and Richards (1980). SMT analysis was based on the seismograms recorded by the underground seismic network and the SMT inversion was performed using FOCI software (Kwiatek, 2016). Three solutions were obtained from the calculations, following the convention introduced by Knopoff and Randall (1970): 1) the full seismic moment tensor is decomposed into an isotropic component (I) which describes the volumetric changes in the source (explosion /+/ or implosion /–/), a compensated linear vector dipole (CLVD) which describes uniaxial compression /–/ or tension /+/, and a double-couple component (DC) which relates to pure shear; 2) the deviatoric tensor which has a CLVD component, a shear DC component and 3) the pure shear tensor, with only the double-couple DC component.

The full, deviatoric, and pure shear moment tensors are calculated using the least-squares approach (L2 norm) as a measure of the misfit. For each mining-induced seismic event, the following parameters were calculated: components of the moment tensor, scalar seismic moment, strike and dip of two nodal plane (A and B), rake, strike and plunge of axis P, T (uncertainties of strike, dip and rake are <15°), percentage of components: I, CLVD, DC, quality coefficient and uncertainty of the tensor.

4.2. Results and discussion

4.2.1. The main trough

The study area, Ziemowit colliery, is located in the center of the main trough. In this area it is assumed that the parameters of the focal mechanism of high-energy tremors reflect the system of stresses within the rock mass, which in turn influences variation in the values of geomechanical parameters in the main trough. The tectonics of the Ziemowit colliery is characterized by a block structure with three groups of fault directions: SW–NE, SE–NW and E–W. The fault throws are between 60 m and 300 m, with rejuvenation of the largest discontinuities having occurred in the Miocene.

Values of geomechanical parameters of the rock mass and coal seams of Group 200 (Łaziskie Beds) and 300 (Orzeskie Beds) were determined from a few dozen borehole samples subjected to laboratory tests, and are presented in Table 2. The foundation of the observed variation in geomechanical properties of the rocks in the area analyzed, with respect to the different tectonic stress fields, are the results of laboratory testing of rock and coal samples from the Łaziskie Beds and Orzeskie Beds. The following geomechanical parameters were tested for: UCS, Young's modulus (E) (static modulus of elasticity) and post-critical modulus (M). These were determined from rock failure curves determined from a universal testing machine (Table 2, Fig. 4). The sampling locations and fault directions (SW–NE, SE–NW and E–W) are shown in Fig. 5.

Data presented in Table 2, separately for the main rock types in the main trough, show that the values of the analyzed geomechanical parameters are different. Relatively high values are

Average geomechanical parameters of rocks in the southern part of the main trough (Ziemowit colliery)

Group of coal seams	Rock types	Areas with only compressive principal stresses			Areas with one principal tensile stress		
		Uniaxial compressive strength (MPa)	Young's modulus (GPa)	Post-critical modulus (GPa)	Uniaxial compressive strength (MPa)	Young's modulus (GPa)	Post-critical modulus (GPa)
Łaziskie Beds No. 200	coal	30.8	2.391	14.615	25.8	2.177	14.096
	sandstone	19.2	2.791	5.367	18.3	2.735	4.820
	mudstone	28.9	1.665	5.803	no data	no data	no data
	claystone	23.5	2.713	9.451	32.7	3.790	8.447
Orzeskie Beds No. 300	coal	25.2	1.949	12.124	21.2	1.872	7.380
	sandstone	no data	no data	no data	32.7	5.074	no data
	claystone	22.8	2.539	7.179	19.2	2.175	6.376
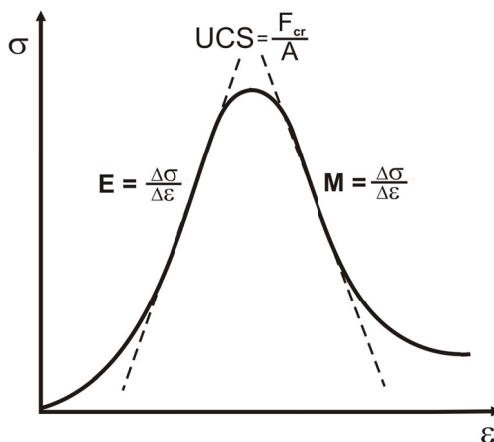
Fig. 4. Idealized stress-strain curve showing the geomechanical parameters: stress (σ), strain (ε), uniaxial compressive strength (*UCS*), critical force (F_{cr}), surface of sample (*A*) and strain increase ($\Delta\varepsilon$). In the pre-critical curve, stress increase is denoted as $\Delta\sigma$ and in the post-critical curve stress decrease is denoted as $\Delta\sigma$, Young's modulus as *E* and post-critical modulus as *M*

evident in areas of tectonic compaction, given that both compressive strength and elastic modulus significantly influence the ability of rocks to develop elastic strain energy. Thus, these parameters influence the intensity of elastic strain energy release during rock mass destruction. This leads to geodynamic phenomena, such as rock bursts, which may occur catastrophically. The regional differences in rock mass properties, which depend on the stress fields and tectonic history of an observed area, are therefore significant.

Ambiguous values of geomechanical parameters were obtained from coal and claystone sample of the Łaziskie Beds. This may have been caused, among other factors, by insufficient data from the area with tensile principal stresses or the lack of data from mudstones in the area. A complete dataset for sandstones and mudstones of the Orzesze Beds is also lacking. Thus, it

is not possible to demonstrate an association between the geomechanical parameters and the tectonic setting.

The distribution of seismic activity is considered to be the result of changes in the values of geomechanical parameters in the study area. The sources of seismic tremors (Fig. 5) appear only in the southeast of the study area, despite the fact that mining activities have been conducted throughout the entire Ziemowit colliery. This area has been previously described as the zone of tectonic compaction (Bukowska, 2009).
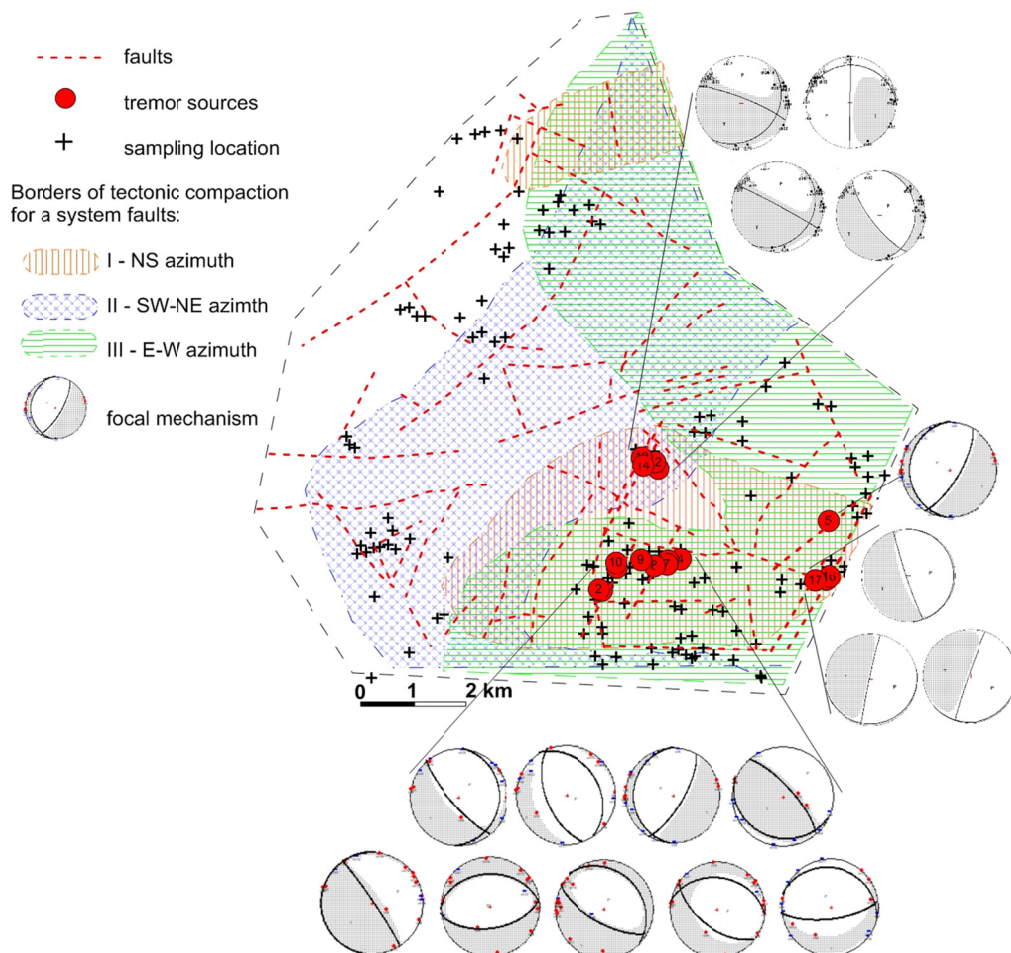
Fig. 5. Map showing the distribution of compaction zones, sampling locations and tremor source mechanisms in relation to tectonic structures in the Ziemowit colliery

Seismic events in the area became a problem in the early 1980s even though mining activities began in the 1960s. The tremors were detected at surface, but no damage was caused to underground workings. For the 17 strong tremors ($E \geq 5 \times 10^6$ J, $M_L \geq 2.6$), which occurred during

exploitation of seams 207 and 209 in the Łaziskie Beds, the focal mechanism was calculated using the seismic SMT method (FOCI software). The calculations were based on seismograms recorded by the seismic network at the Ziemowit colliery (Gołda et al., 2015). During the research, the seismic network consisted of 16 vertical Willmore seismometers (Sensonics Ltd., Hertfordshire, United Kingdom) located underground, at the depths of the coal seams. The recording seismometers are horizontally and vertically spaced from seismic events at distances in the 0.3-5 km range and 0.1-0.8 km range, respectively. Constant values of velocity (4000 m/s) and density (2300 kg/m^3) were selected for the study, and the accuracy of focal mechanism determination was controlled using the solution quality factor Q, which can be in the 0-100% range, and was chosen for the lowest value of uncertainty denoted by ERR. Results for $Q < 40\%$ were discarded.

The investigated tremors revealed a slip mechanism (Table 3, Fig. 5), and the full tensor mainly contained up to 23% of the isotropic component (I), up to 20% uniaxial compression or tension (CLVD), and approximately 66-89% of the shear component (DC). Compressive stresses (P) were typically more vertically oriented than tensile stresses (T). The strike of one of the nodal planes is within 20° of the strike value of the tectonic faults.

TABLE 3

List of focal mechanism parameters of tremors ($E \geq 5 \times 10^6$ J, $M_L \geq 2.6$) in the main trough of the Ziemowit colliery in the 2007-2016 period

No Tremor	Date Time	Energy (J)	*Nodal plane		Stresses		Full tensor Components (%)			Focal mechanism	
			A $\Phi°/\delta°$ $\lambda°$	B $\Phi°/\delta°$ $\lambda°$	P $\Phi°/\delta°$	T $\Phi°/\delta°$	I	CLVD	DC		
1	2008-10-07 21:41	7×10^6	122/83 −94	333/8 −59	27/52	216/38	23	2	75		RE
2	2008-10-24 11:55	8×10^6	323/73 −85	127/17 −106	240/61	49/28	−12	−11	77		RE
3	2009-11-17 3:46	5×10^7	359/86 79	250/12 161	257/48	99/40	−6	20	74		NO
4	2010-02-27 3 :41	7×10^6	71/77 96	224/14 65	155/32	348/57	19	15	66		NO
5	2010-03-12 22:50	9×10^6	30/71 −81	182/21 −116	314/62	112/26	−5	−3	92		NO
6	2010-11-08 11:28	8×10^6	82/54 −93	267/36 −86	337/81	174/9	9	2	89		NO
7	2010-11-12 14:02	9×10^6	114/68 −107	320/23 −66	6/66	212/22	20	4	76		NO
8	2010-12-23 2:10	8×10^6	228/72 −116	105/31 −37	105/56	338/22	20	6	74		NO

TABLE 3. CONTINUED

9	2011-02-08 15:14	$7×10^6$	116/59 66	337/38 124	341/66	223/11	−18	−19	63		NO
10	2011-05-12 15:09	$7×10^6$	162/61 −75	312/33 −115	106/70	240/14	−16	−20	64		NO
11	2014-04-18 19:33	$1×10^7$	1/90 −110	271/20 0	252/42	110/42	−17	11	72		NO
12	2014-05-19 06:29	$2×10^6$	143/73 −105	6/23 −49	32/59	245/26	−6	−1	83		NO
13	2014-06-27 14:37	$5×10^6$	300/88 114	34/24 6	7/38	232/43	17	17	66		NO
14	2014-07-17 04:01	$9×10^6$	292/80 114	43/25 23	2/31	227/49	22	5	73		NO
15	2015-05-07 03:44	$2×10^7$	199/87 −92	52/4 −58	107/48	291/42	−10	−7	83		NO
16	2015-05-17 06:20	$5×10^6$	192/88 −95	77/5 −25	97/47	286/43	−8	−7	85		NO
17	2016-11-21 17:28	$8×10^6$	162/86 −91	356/4 −76	71/49	253/41	−15	−13	72		NO
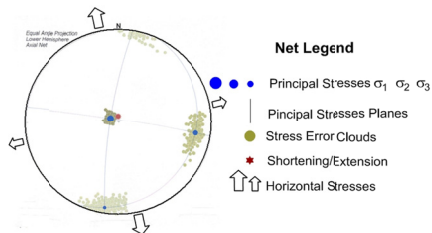
* Φ – strike of nodal plane A or B; δ – dip of nodal plane A or B; λ – slip angle; Φ – trend axis of P or T; δ – plunge axis of P or T; I – percentage of isotropic component; CLVD – percentage of compensated linear vector dipole component where compression is negative (–) and tension is positive (+); DC – percentage of shear component (double-couple); NO – normal slip mechanism; RE – reverse slip mechanism.

The stress calculations were performed using 17 events (Table 3) based on the strike and dip angle of the selected nodal plane. The relative sizes of the three principal stresses are related to the faulting mechanism of a region, and thus characterization of a region with respect to normal faulting can be done by defining the size of the two horizontal stresses relative to the vertical. The best-fit principal stresses σ_1, σ_2 and σ_3 are shown in Table 4.

The resulting stress tensor in Table 4 shows an extensional regime with σ_1 nearly vertical and σ_2 and σ_3 nearly horizontal. The value of the stress ratio R is 0.17, which corresponds to a normal faulting regime. The mean misfit angle of 6±4° indicates good consistency between the focal mechanism and the resolved stress tensor (Gephart & Forsyth, 1984). The value of relative maximum shear stress is 0.31, with a friction angle of 29°. The horizontal stress marked in Table 4 with white arrows is tensile stress, with extension in a NNW–SSE direction. The axis of shortening/extension, which is the direction of strain in a given region, is nearly vertical in orientation. This type of stress state, with the maximum principal stress directed vertically, cor-responds to typical conditions in the rock mass, and reflects the influence of overlying strata

Stress tensor inversion results for tremors ($E \geq 5 \times 10^6$ J, $M_L \geq 2.6$) in the main trough
of the Ziemowit colliery in the period 2007-2016

Stereoplot

Net Legend

- Principal Stresses σ_1 σ_2 σ_3
- Pincipal Stresses Planes
- Stress Error Clouds
- Shortening/Extension
- Horizontal Stresses

Parameters	Value
maximum stress axis, σ_1	297°/79°
intermediate stress axis, σ_2	99°/11°
minimum stress axis, σ_3	189°/3°
stress ratio, R	0.17
mean misfit angle ± std. deviation	6±4°
mean fault angle ± std. deviation	12.3° ± 9.2°
mean friction angle, Φ	29°
mean shear stress, τ ± std. deviation	0.31 ± 0.01
shortening/extension (trend/plunge)	355°/82°

which yield to cracking and failure during mining advancement. An additional factor of the high seismicity is the influence of mine workings on the destruction of faults in the zone of tectonic compaction (Bukowska, 2009).

4.2.2. The Upper Silesian fold series – Bytom trough

The Bytom trough is located in a tectonic compaction zone (Fig. 6). It is a relatively shallow, asymmetric syncline consisting of a number of shallow synclines separated by elevated domes that strike NW–SE. The axis of the trough has a longitudinal E–W strike, close to the NE branch dip angle of the layers with values of 8-20°. Dip angles in the southern branch do not exceed 3°. The structure of the trough has also been disturbed by a network of predominantly NW–SE striking faults, and faults perpendicular to this direction. The fault throws vary between a few meters and nearly 300 m, accompanied by a network of faults with lower throw distances (dozen centimeters up to ~20 m).

Very high seismic activity has been observed in the area, with more than 28530 tremors of energy $E \geq 10^5$ J ($M_L \geq 1.7$) recorded between 1977 and 2016 and nine events of energy $E \geq 10^8$ J ($M_L \geq 3.3$) recorded over the same period. The source of the tremors with energy $>10^8$ J is located in the axis of the trough at a depth of a few hundred meters below the mining activities. The data presented by Marcak and Mutke (2013) concerned the analysis of two tremors $>10^8$ J. The foci of the tremors were located in the area of wall 3 in seam 503 (saddle layer) in the Bobrek-Centrum colliery, located at the base of the Bytom trough. These results were confirmed by other researchers as well (Kozłowska et al., 2016). To determine the location of the hypo-

176

centers, researchers have used the macroseismic distribution of ground vibration intensity and analysis of tremor seismograms. Such investigation has shown that the tremors were generated by tectonic stresses, and the stresses imposed by mining activities simply provided the impulse to trigger the release of the elastic strain energy accumulated in the rock mass.

To characterize the stress field in the study area, the parameters of the focal mechanism of a few of the strongest tremors ($E \geq 10^6$, $M_L \geq 2.2$) that occurred along the axis of the Bytom trough are presented in this paper for the period 2007-2016 (Table 5, Fig. 7). The full moment tensor solution shows that the tremors occurred during reverse faulting, with dominant shear component (DC) in the focal mechanism, an isotropic component (I) and compensated linear vector dipole (CLVD). The nodal planes have an approximate NW–SE azimuth, and compressive stresses (P) in the source are almost horizontal with NE–SW azimuths, and tensile stresses (T) are nearby vertical with NW–SE azimuths.

TABLE 5

List of focal mechanism parameters of tremors ($E \geq 8 \times 10^6$ J, $M_L \geq 2.7$) in the Bytom trough of the Bobrek-Centrum colliery for the period 2007-2016

Date Time	Energy (J)	*Nodal planes		Stresses		Full tensor components (%)			Focal mechanism	
		A $\Phi°/\delta°$ $\lambda°$	B $\Phi°/\delta°$ $\lambda°$	P $\Phi°/\delta°$	T $\Phi°/\delta°$	I	CLVD	DC		
2007-02-09 14:45	1×10^9	171/56	320/38	248/9	127/72	–3	–6	91		RE
2008-12-19 23:45	7×10^8	326/58	123/34	47/12	270/73	10	3	87		RE
2009-12-16 03:06:35	8×10^8	339/53 96	149/37 82	64/8	276/81	–7	5	88		RE
2010-02-05 11:59:14	1×10^7	326/62 106	115/32 63	45/15	269/69	14	10	76		RE
2010-03-02 0:06:38	8×10^6	140/60 63	6/39 129	3/11	249/64	13	13	74		RE
2010-03-11 1:07:16	9×10^6	351/52 120	127/47 57	60/3	323/66	13	10	77		RE
2016-06-03 08:42:05	3×10^8	122/90 110	213/20 2	194/41	51/42	–32	2	66		RE

* Φ – strike of nodal plane A or B; δ – dip of nodal plane A or B; λ – slip angle; Φ – trend axis of P or T; δ – plunge axis of P or T; I – percentage of isotropic component; CLVD – percentage of compensated linear vector dipole component where compression is negative (–) and tension is positive (+); DC – percentage of shear component (double-couple); NO – normal slip mechanism; RE – reverse slip mechanism.
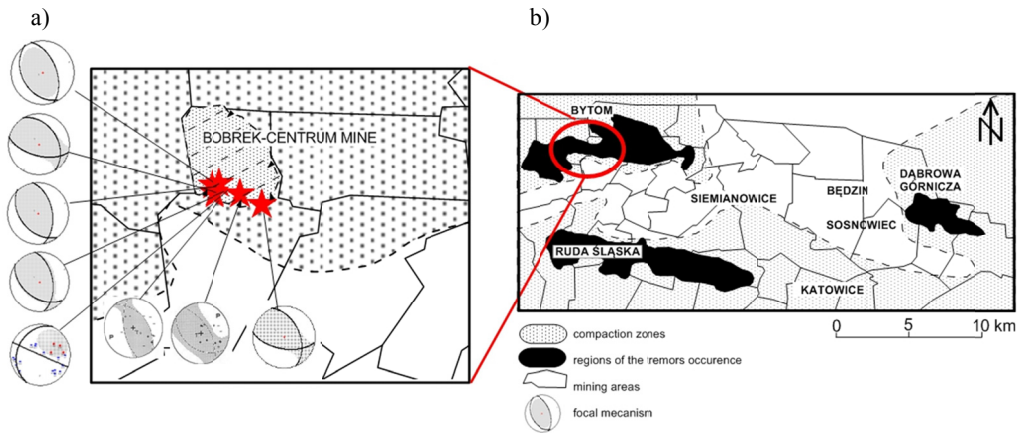
Fig. 7. Maps showing (a) tremor source mechanisms in the Bytom trough and (b) the zone of tectonic compaction in the northern part of USCB (after Goszcz, 1985)

As shown in Table 6, the distribution of stresses determined from the focal mechanism parameters was as follows: σ_1 and σ_2 were generally horizontally oriented, while σ_3 was vertical. The value of relative maximum shear stress was 0.44, and the internal friction angle (Φ) was 34°. The horizontal stress was compressive, with a NE–SW azimuth. The axis of shortening/extension had a NE–SW azimuth and was nearly horizontally oriented. This type of stress, with

TABLE 6

Stress tensor inversion results for tremors ($E \geq 8 \times 10^6$ J, $M_L \geq 2.7$) in the Bytom trough of the Bobrek-Centrum colliery for the 2007–2016 period

Parameters	Value
maximum stress axis, σ_1	239°/4°
intermediate stress axis, σ_2	148°/7°
minimum stress axis, σ_3	360°/81°
stress ratio, R	0.31
mean misfit angle ± std. deviation	3° ± 2°
mean fault angle ± std. deviation	37±12°
mean friction angle, Φ	34°
mean shear stress, τ ± std. deviation	0.44 ± 0.002
shortening/extension (trend/plunge)	244°/19°

horizontal σ_1, reflects conditions influenced by tectonic stresses within the axis of the trough triggered by mining activities (Marcak & Mutke, 2013). Based on the results of focal mechanism and local stress field analysis in the Bytom trough it can be concluded that the system of stresses active in the foci of the tremors is similar to the stresses determined for the state of strain in the rock mass during Alpine orogenesis. These results are comparable to the results of structural analysis conducted by Teper (1998). The directions of compressive stress P and tensile stresses T in the tremor's source reflect the directions of compression and tension, respectively, determined tectonophysically. Finally, the strike directions of reverse faults in the area are similar to the azimuths of nodal planes determined from the solution of the focal mechanism.

The analyses conducted show that the focal mechanism of a high-energy tremor roughly reflects the system of tectonic stresses that occur in the rock mass, which in turn influences the different values of geomechanical parameters of the rocks. The changes in geomechanical properties in the analyzed area of the USCB were assessed via laboratory testing of rock samples and coal from saddle beds, and take the occurrence of different tectonic stress fields into consideration. The following parameters were analyzed from laboratory tests in a servo-controlled testing machine: UCS, static elasticity modulus, and post-peak failure modulus of coal. The values of these parameters were determined from a failure curve (Table 7) characteristic of compaction zones (Bukowska, 2009).

TABLE 7

Average geomechanical parameters of rocks in the Upper Silesian Fold Zone (Bytom trough) from boreholes B-8, G-171, 38/9, and V39/5

Group of seams	Rocks	Areas in a compressional regime		
		Uniaxial compressive strength (MPa)	Young's modulus (GPa)	Post critical modulus (GPa)
Siodłowe Beds No. 500	coal	28.2	2.151	12.021
	sandstone	57.5	6.644	no data
	claystone	45.5	5.301	no data

5. Conclusions

The Carboniferous rock mass in the USCB has a complex geological structure, in terms of both stratigraphic profile and tectonic history. The tectonic history of the USCB has been predominantly the result of the Leonian phase of Variscan orogenesis, along with rejuvenation of structures during more recent Alpine orogenesis.

The tectonic structures were formed as a result of tectonic stresses, contributing to shaping areas of compression in which the components of principal stresses were compressive, and areas in which principal stresses were tensile. Such a distribution of principal stresses in the rock mass may have contributed to variation in values of important geomechanical parameters of rocks, an issue that has been researched very little.

Research into the regularity of changes in geomechanical properties of the rocks of the Upper Carboniferous in USCB requires further attention to be able to resolve problems associated with geodynamic phenomena occurring in the rock mass. This is because such phenomena, including seismic tremors and rockbursts, depend strongly on the distribution of tectonic stress

fields. Additionally, seismic activity in the Carboniferous rock mass is caused by local stress fields controlled by tectonic structure, and mining-related stresses.

Finally, to better explain the changes evident in geomechanical properties of the rocks responsible for high-energy tremors in the research area, the stress fields in both the main trough and Bytom trough were calculated from analysis of the focal mechanism parameters.

Acknowledgements

References

Aki K., Richards P.G., 1980. *Quantitative Seismology – Theory and Methods*. San Francisco, WH Freeman.

Anderson E.M., 1951. *The Dynamics of Faulting*. Oliver & Boyd.

Angelier J., 2002. *Inversion of earthquake focal mechanisms to obtain the seismotectonic stress IV – a new method free of choice among nodal lines*. Geophys. J. Int. **150**, 588-609.

Arnold R., Townend J., 2007. *A Bayesian approach to estimating tectonic stress from seismological data*. Geophys. J. Int. **170**, 3, 1336-1356. DOI: 10.1111/j.1365-246X.2007.03485.x.

Bukowska M., (ed.), 2009. *A Complex Method for Assessing Susceptibility to Rock Bumps in the Upper Silesian Coal Basin*. GIG, Katowice, in Polish.

Bukowska M., 2012. *The rockbursts in the Upper Silesian Coal Basin in Poland.* Journal of Mining Science **48**, 3, 445-456. DOI: 10.1134/S1062739148030070.

Bukowski P., Augustyniak I., 2013. *Changes in the structure of water inflow into coal mines in Poland*. 13th International Multidisciplinary Scientific Geoconference on "Geoconference on Science and Technologies in Geology, Exploration and Mining SGEM". Albena, Bulgaria. VOL II, Book Series: International Multidisciplinary Scientific GeoConference-SGEM, 25-32.

Bukowski P., 2015. *Evaluation of water hazard in hard coal mines in changing conditions of functioning of mining industry in Upper Silesian Coal Basin – USCB (Poland)*. Arch. Min. Sci. **60**, 2, 455-475.

Buła Z., Żaba J., Habryn R., 2008. *Rejonizacja tektoniczna Polski – Polska południowa (blok górnośląski i blok małopolski) (Tectonic regionalization of Poland – Southern Poland (Upper Silesian Block, Małopolska Block))*. Przegląd Geologiczny **56**, 10, 912-920, in Polish.

Dubiński J., Wierzchowska Z., 1973. *Metody obliczeń energii wstrząsów górotworu na Górnym Śląsku*. Prace GIG, Komunikat nr 591, Katowice, in Polish.

Fojtíková L., Vavryčuk V., Cipciar A., Madarás J., 2010. *Focal mechanisms of micro-earthquakes in the Dobrá Voda seismoactive area in the Malé Karpaty Mts. (Little Carpathians), Slovakia*. Tectonophys. **492**, 1213-229.

Gephart J.W., Forsyth D.W., 1984. *An improved method for determining the regional stress tensor using earthquake focal mechanism data: application to the San Fernando earthquake sequence*. J. Geophys. Res. **89**, 9305-9320.

Gołda A., Śladowski G., Wieczorek K., 2015. *Mechanizmy ognisk wstrząsów górniczych zarejestrowanych w trakcie eksploatacji pokładu 209 ścianą 911 w bloku D KWK „Ziemowit"*. Czasopismo Naukowo-Techniczne Górnictwa Rud **1**, 74, 67-82, in Polish.

Goszcz A., 1980. *Wpływ napięć tektonicznych na niektóre własności skał i warunki górnicze w północno-wschodniej części Górnośląskiego Zagłębia Węglowego (Influence of tectonic stresses on certain properties of rocks and mining conditions in the Northeastern part of Upper Silesian Coal Basin)*. Zesz. Nauk. AGH, Geologia **27**, 9-92, in Polish.

Goszcz A., 1985. *Kompakcja tektoniczna jako przyczyna naturalnej skłonności skał do wstrząsów górniczych i tąpań (Tectonic compaction as the natural cause the proneness of rockbursts)*. Przegląd Górniczy **7-8**, 239-244, in Polish.

180

Goszcz A., Dworak J., 1982. *Określenie skłonności do tąpań na podstawie analizy tektonofizycznej oraz parametrów sprężystych pokładu metodą sejsmiczną w wyrobiskach górniczych (Determining bump susceptibility in mine workings with a seismic method based on tectonophysical analysis and elastic parameters of a seam)*. Archiwum Górnictwa **27**, 1-2, 45-56, in Polish.

Gzowskij M.W., 1975. *Osnowy tektonofiziki*. Nauka, in Russian.

Hofstetter A., Dorbath C., Dorbath L., Braeuer B., Weber M., 2016. *Stress tensor and focal mechanisms in the Dead Sea basin*. J. Seism. **20**, 2, 669-699.

Kabiesz J., 2016. *Koincydencja górniczych zagrożeń naturalnych*. Wyd. GIG, Katowice, ISBN 987-83-65503-00-8.

Kisiel L., 1973. *Reologia skał. Podstawy Naukowe*. Wyd. Ossolineum, in Polish.

Knopoff L., Randall M.J., 1970. *The compensated linear-vector dipole. A possible mechanism for deep earthquakes*. J. Geophys. Res. **75**, 1957-1963.

Kotas A., 1982. *Zarys budowy geologicznej Górnośląskiego Zagłębia Węglowego (Outline of geology of Upper Silesia Coal Basin)*. Przewodnik LIV Zjazdu PTG. Warszawa. Wyd. Geologiczne, 45-73, in Polish.

Kozłowska M., Orlecka-Sikora B., Rudziński Ł., Cielesta S., Mutke G., 2016. *Atypical evolution of seismicity patterns resulting from the coupled natural, human-induced and coseismic stresses in a longwall coal mining environment*. Int. J. Rock Mech. and Min. Sci. **86**, 5-15, DOI: 10.1016/j.ijrmms.2016.03.024.

Kwiatek G., Martínez-Garzón P., Bohnhoff M., 2016. *HybridMT: A MATLAB/shell environment package for seismic moment tensor inversion and refinement*. Seismol. Res. Lett. **87**, 4, 964-976, DOI:10.1785/0220150251.

Lurka A., Stec K., 2015. *Charakterystyka i sejsmologiczne metody analizy aktywności sejsmicznej Górnośląskiego Zagłębia Węglowego*. Przegląd Górniczy **1**, 83-93, in Polish.

Marcak H., Mutke G., 2013. *Seismic activation of tectonic stresses by mi*ning. J. Seism. **17**, 4, 1139-1148, DOI:10.1007/s10950-013-9382-3.

McKenzie D., 1969. *The relation between fault plane solutions for earthquakes and the directions of the principal stresses*. Bull. Seismol. Soc. Amer. **59**, 591-601.

Michael A.J., 1987. *Use of focal mechanisms to determine stress: a control study*. J. Geophys. Res. **92**, B1, 357-368.

Reches Z., 1987. *Determination of the tectonic stress tensor from slip along faults that obey the Coulomb yield condition*. Tectonics **6**, 6, 849-861.

Sanford A.R., 1959. *Analytical and experimental study of simple geologic structures*. Geol. Soc. Amer. Bull. **70**, 1, 19-52.

Stec K., 2007. *Characteristics of seismic activity of the Upper Silesian coal basin in Poland*. Geophys. J. Int. **168**, 2, 757-768, DOI: 10.1111/j.1365-246X.2006.03227.x.

Stec K., 2012. *Focal mechanisms of mine-induced seismic events an explanation of geomechanical processes in the area of longwall 6, seam 510 in hard coal mine "Bobrek-Centrum"*. Arch. Min. Sci. **57**, 4, 871-886, DOI: 10.2478/v10267-012-0057-7.

Stec K., 2015. *Geomechanical conditions of causes of high-energy rock mass tremors determined based on the analysis focal mechanisms*. J. Sust. Min. **1**, 55-65, DOI:org/10.1016/j.jsm.2015.08.008.

Teper L., 1998. *Wpływ nieciągłości podłoża karbonu na sejsmotektonikę północnej części Górnośląskiego Zagłębia Węglowego (Influence of discontinuities in Carboniferous bed on seismotectonics of the northern part of Upper Silesia Coal Basin)*. Wyd. Uniwersytetu Śląskiego, Katowice, in Polish.

Vavryčuk V., 2014. *Iterative joint inversion for stress and fault orientations from focal mechanisms*. Geophys. J. Int. **199**, 1, 69-77. DOI:10.1093/gji/ggu224.